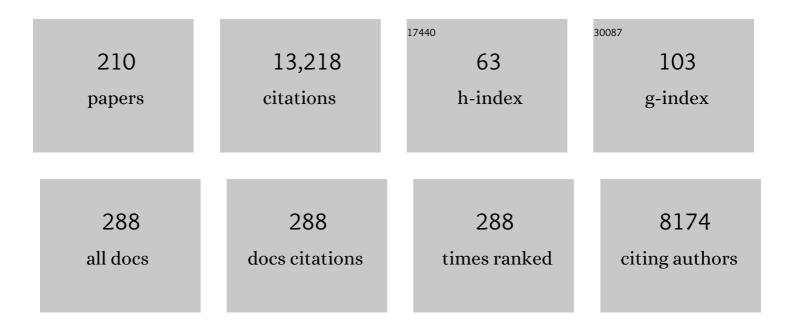
## Nickolay A Krotkov

List of Publications by Year in descending order

Source: https://exaly.com/author-pdf/560288/publications.pdf Version: 2024-02-01



#	Article	IF	CITATIONS
1	Aura OMI observations of regional SO <sub>2</sub> and NO <sub>2</sub> pollution changes from 2005 to 2015. Atmospheric Chemistry and Physics, 2016, 16, 4605-4629.	4.9	521
2	Emissions estimation from satellite retrievals: A review of current capability. Atmospheric Environment, 2013, 77, 1011-1042.	4.1	323
3	A decade of global volcanic SO2 emissions measured from space. Scientific Reports, 2017, 7, 44095.	3.3	289
4	A new stratospheric and tropospheric NO <sub>2</sub> retrieval algorithm for nadir-viewing satellite instruments: applications to OMI. Atmospheric Measurement Techniques, 2013, 6, 2607-2626.	3.1	269
5	The Ozone Monitoring Instrument: overview of 14 years in space. Atmospheric Chemistry and Physics, 2018, 18, 5699-5745.	4.9	259
6	Band residual difference algorithm for retrieval of SO/sub 2/ from the aura ozone monitoring instrument (OMI). IEEE Transactions on Geoscience and Remote Sensing, 2006, 44, 1259-1266.	6.3	253
7	Tropospheric emissions: Monitoring of pollution (TEMPO). Journal of Quantitative Spectroscopy and Radiative Transfer, 2017, 186, 17-39.	2.3	239
8	SO <sub>2</sub> emissions and lifetimes: Estimates from inverse modeling using in situ and global, space-based (SCIAMACHY and OMI) observations. Journal of Geophysical Research, 2011, 116, .	3.3	230
9	India Is Overtaking China as the World's Largest Emitter of Anthropogenic Sulfur Dioxide. Scientific Reports, 2017, 7, 14304.	3.3	230
10	Volcanic sulfur dioxide measurements from the total ozone mapping spectrometer instruments. Journal of Geophysical Research, 1995, 100, 14057.	3.3	217
11	Highâ€Resolution Mapping of Nitrogen Dioxide With TROPOMI: First Results and Validation Over the Canadian Oil Sands. Geophysical Research Letters, 2019, 46, 1049-1060.	4.0	209
12	Abrupt decline in tropospheric nitrogen dioxide over China after the outbreak of COVID-19. Science Advances, 2020, 6, eabc2992.	10.3	208
13	A global catalogue of large SO <sub>2</sub> sources and emissions derived from the Ozone Monitoring Instrument. Atmospheric Chemistry and Physics, 2016, 16, 11497-11519.	4.9	200
14	The version 3 OMI NO <sub>2</sub> standard product. Atmospheric Measurement Techniques, 2017, 10, 3133-3149.	3.1	198
15	Distribution of UV radiation at the Earth's surface from TOMS-measured UV-backscattered radiances. Journal of Geophysical Research, 1999, 104, 12059-12076.	3.3	196
16	Retrieval of large volcanic SO <sub>2</sub> columns from the Aura Ozone Monitoring Instrument: Comparison and limitations. Journal of Geophysical Research, 2007, 112, .	3.3	186
17	Satellite data of atmospheric pollution for U.S. air quality applications: Examples of applications, summary of data end-user resources, answers to FAQs, and common mistakes to avoid. Atmospheric Environment, 2014, 94, 647-662.	4.1	186
18	Evaluation of OMI operational standard NO <sub>2</sub> column retrievals using in situ and surface-based NO <sub>2</sub> observations. Atmospheric Chemistry and Physics, 2014, 14, 11587-11609.	4.9	182

#	Article	IF	CITATIONS
19	Satellite estimation of spectral surface UV irradiance in the presence of tropospheric aerosols: 1. Cloud-free case. Journal of Geophysical Research, 1998, 103, 8779-8793.	3.3	177
20	Scaling Relationship for NO <sub>2</sub> Pollution and Urban Population Size: A Satellite Perspective. Environmental Science & Technology, 2013, 47, 7855-7861.	10.0	176
21	What would have happened to the ozone layer if chlorofluorocarbons (CFCs) had not been regulated?. Atmospheric Chemistry and Physics, 2009, 9, 2113-2128.	4.9	165
22	A fast and sensitive new satellite SO <sub>2</sub> retrieval algorithm based on principal component analysis: Application to the ozone monitoring instrument. Geophysical Research Letters, 2013, 40, 6314-6318.	4.0	165
23	U.S. NO2 trends (2005–2013): EPA Air Quality System (AQS) data versus improved observations from the Ozone Monitoring Instrument (OMI). Atmospheric Environment, 2015, 110, 130-143.	4.1	162
24	Lifetimes and emissions of SO <sub>2</sub> from point sources estimated from OMI. Geophysical Research Letters, 2015, 42, 1969-1976.	4.0	152
25	Estimation of SO <sub>2</sub> emissions using OMI retrievals. Geophysical Research Letters, 2011, 38, n/a-n/a.	4.0	150
26	Space-based detection of missing sulfur dioxide sources of global air pollution. Nature Geoscience, 2016, 9, 496-500.	12.9	149
27	Recent large reduction in sulfur dioxide emissions from Chinese power plants observed by the Ozone Monitoring Instrument. Geophysical Research Letters, 2010, 37, .	4.0	147
28	Tracking volcanic sulfur dioxide clouds for aviation hazard mitigation. Natural Hazards, 2009, 51, 325-343.	3.4	141
29	Validation of SO <sub>2</sub> retrievals from the Ozone Monitoring Instrument over NE China. Journal of Geophysical Research, 2008, 113, .	3.3	139
30	Structural uncertainty in air mass factor calculation for NO <sub>2</sub> and HCHO satellite retrievals. Atmospheric Measurement Techniques, 2017, 10, 759-782.	3.1	133
31	Improved satellite retrievals of NO <sub>2</sub> and SO <sub>2</sub> over the Canadian oil sands and comparisons with surface measurements. Atmospheric Chemistry and Physics, 2014, 14, 3637-3656.	4.9	132
32	Validation of daily erythemal doses from Ozone Monitoring Instrument with groundâ€based UV measurement data. Journal of Geophysical Research, 2007, 112, .	3.3	129
33	Photomineralization of terrigenous dissolved organic matter in Arctic coastal waters from 1979 to 2003: Interannual variability and implications of climate change. Global Biogeochemical Cycles, 2006, 20, n/a-n/a.	4.9	126
34	Satellite observations of changes in air quality during the 2008 Beijing Olympics and Paralympics. Geophysical Research Letters, 2009, 36, .	4.0	120
35	Air quality over the Canadian oil sands: A first assessment using satellite observations. Geophysical Research Letters, 2012, 39, .	4.0	120
36	Sulfur dioxide emissions from Peruvian copper smelters detected by the Ozone Monitoring Instrument. Geophysical Research Letters, 2007, 34, .	4.0	119

#	Article	IF	CITATIONS
37	Daily monitoring of Ecuadorian volcanic degassing from space. Journal of Volcanology and Geothermal Research, 2008, 176, 141-150.	2.1	113
38	Ozone Monitoring Instrument Observations of Interannual Increases in SO <sub>2</sub> Emissions from Indian Coal-Fired Power Plants during 2005–2012. Environmental Science & Technology, 2013, 47, 13993-14000.	10.0	113
39	Earth Observations from DSCOVR EPIC Instrument. Bulletin of the American Meteorological Society, 2018, 99, 1829-1850.	3.3	108
40	Satellite estimation of spectral surface UV irradiance: 2. Effects of homogeneous clouds and snow. Journal of Geophysical Research, 2001, 106, 11743-11759.	3.3	106
41	Retrieval of vertical columns of sulfur dioxide from SCIAMACHY and OMI: Air mass factor algorithm development, validation, and error analysis. Journal of Geophysical Research, 2009, 114, .	3.3	105
42	Enhanced Capabilities of TROPOMI NO <sub>2</sub> : Estimating NO <sub><i>X</i></sub> from North American Cities and Power Plants. Environmental Science & Technology, 2019, 53, 12594-12601.	10.0	103
43	Application of OMI, SCIAMACHY, and GOMEâ€₂ satellite SO <sub>2</sub> retrievals for detection of large emission sources. Journal of Geophysical Research D: Atmospheres, 2013, 118, 11,399.	3.3	102
44	Fog―and cloudâ€induced aerosol modification observed by the Aerosol Robotic Network (AERONET). Journal of Geophysical Research, 2012, 117, .	3.3	99
45	The observed response of Ozone Monitoring Instrument (OMI) NO2 columns to NOx emission controls on power plants in the United States: 2005–2011. Atmospheric Environment, 2013, 81, 102-111.	4.1	99
46	Surface ultraviolet irradiance from OMI. IEEE Transactions on Geoscience and Remote Sensing, 2006, 44, 1267-1271.	6.3	98
47	Aircraft observations of dust and pollutants over northeast China: Insight into the meteorological mechanisms of transport. Journal of Geophysical Research, 2007, 112, .	3.3	98
48	Hit from both sides: tracking industrial and volcanic plumes in Mexico City with surface measurements and OMI SO <sub>2</sub> retrievals during the MILAGRO field campaign. Atmospheric Chemistry and Physics, 2009, 9, 9599-9617.	4.9	96
49	Dispersion and lifetime of the SO <sub>2</sub> cloud from the August 2008 Kasatochi eruption. Journal of Geophysical Research, 2010, 115, .	3.3	91
50	Impacts of brown carbon from biomass burning on surface UV and ozone photochemistry in the Amazon Basin. Scientific Reports, 2016, 6, 36940.	3.3	90
51	Global fine-scale changes in ambient NO2 during COVID-19 lockdowns. Nature, 2022, 601, 380-387.	27.8	90
52	Ozone Monitoring Instrument (OMI) Aura nitrogen dioxide standard product version 4.0 with improved surface and cloud treatments. Atmospheric Measurement Techniques, 2021, 14, 455-479.	3.1	89
53	Comparison of Brewer ultraviolet irradiance measurements with total ozone mapping spectrometer satellite retrievals. Optical Engineering, 2002, 41, 3051.	1.0	88
54	Comparison of daily UV doses estimated from Nimbus 7/TOMS measurements and ground-based spectroradiometric data. Journal of Geophysical Research, 2000, 105, 5059-5067.	3.3	87

Νιςκοίας Α Κrotkov

#	Article	IF	CITATIONS
55	Volcanic eruption detection by the Total Ozone Mapping Spectrometer (TOMS) instruments: a 22-year record of sulphur dioxide and ash emissions. Geological Society Special Publication, 2003, 213, 177-202.	1.3	84
56	UV index climatology over the United States and Canada from ground-based and satellite estimates. Journal of Geophysical Research, 2004, 109, n/a-n/a.	3.3	80
57	Sulfur dioxide vertical column DOAS retrievals from the Ozone Monitoring Instrument: Global observations and comparison to groundâ€based and satellite data. Journal of Geophysical Research D: Atmospheres, 2015, 120, 2470-2491.	3.3	79
58	Direct retrieval of sulfur dioxide amount and altitude from spaceborne hyperspectral UV measurements: Theory and application. Journal of Geophysical Research, 2010, 115, .	3.3	78
59	New-generation NASA Aura Ozone Monitoring Instrument (OMI) volcanic SO <sub>2</sub> dataset: algorithm description, initial results, and continuation with the Suomi-NPP Ozone Mapping and Profiler Suite (OMPS). Atmospheric Measurement Techniques. 2017. 10. 445-458.	3.1	78
60	Spatially and seasonally resolved estimate of the ratio of organic mass to organic carbon. Atmospheric Environment, 2014, 87, 34-40.	4.1	76
61	Assessment of TOMS UV bias due to absorbing aerosols. Journal of Geophysical Research, 2005, 110, .	3.3	73
62	Ozone Monitoring Instrument spectral UV irradiance products: comparison with ground based measurements at an urban environment. Atmospheric Chemistry and Physics, 2009, 9, 585-594.	4.9	73
63	Revising the slant column density retrieval of nitrogen dioxide observed by the Ozone Monitoring Instrument. Journal of Geophysical Research D: Atmospheres, 2015, 120, 5670-5692.	3.3	72
64	A new approach to correct for absorbing aerosols in OMI UV. Geophysical Research Letters, 2009, 36, .	4.0	71
65	Detection of volcanic ash clouds from Nimbus 7/total ozone mapping spectrometer. Journal of Geophysical Research, 1997, 102, 16749-16759.	3.3	68
66	Retrieval of aerosol single scattering albedo at ultraviolet wavelengths at the T1 site during MILAGRO. Atmospheric Chemistry and Physics, 2009, 9, 5813-5827.	4.9	68
67	Measurements of nitrogen dioxide total column amounts using a Brewer double spectrophotometer in direct Sun mode. Journal of Geophysical Research, 2006, 111, .	3.3	66
68	Effect of particle non-sphericity on satellite monitoring of drifting volcanic ash clouds. Journal of Quantitative Spectroscopy and Radiative Transfer, 1999, 63, 613-630.	2.3	65
69	Global satellite analysis of the relation between aerosols and short-lived trace gases. Atmospheric Chemistry and Physics, 2011, 11, 1255-1267.	4.9	65
70	Global dry deposition of nitrogen dioxide and sulfur dioxide inferred from spaceâ€based measurements. Global Biogeochemical Cycles, 2014, 28, 1025-1043.	4.9	65
71	Spectral properties of backscattered UV radiation in cloudy atmospheres. Journal of Geophysical Research, 2004, 109, .	3.3	63
72	Stratospheric Injection of Massive Smoke Plume From Canadian Boreal Fires in 2017 as Seen by DSCOVRâ€EPIC, CALIOP, and OMPS‣P Observations. Journal of Geophysical Research D: Atmospheres, 2020, 125, e2020JD032579.	3.3	63

#	Article	IF	CITATIONS
73	Dry Deposition of Reactive Nitrogen From Satellite Observations of Ammonia and Nitrogen Dioxide Over North America. Geophysical Research Letters, 2018, 45, 1157-1166.	4.0	62
74	A new global anthropogenic SO <sub>2</sub> emission inventory for the last decade: a mosaic of satellite-derived and bottom-up emissions. Atmospheric Chemistry and Physics, 2018, 18, 16571-16586.	4.9	61
75	Measuring global volcanic degassing with the Ozone Monitoring Instrument (OMI). Geological Society Special Publication, 2013, 380, 229-257.	1.3	60
76	Extending the longâ€ŧerm record of volcanic SO <sub>2</sub> emissions with the Ozone Mapping and Profiler Suite nadir mapper. Geophysical Research Letters, 2015, 42, 925-932.	4.0	58
77	Comparison of TOMS and AVHRR volcanic ash retrievals from the August 1992 eruption of Mt. Spurr. Geophysical Research Letters, 1999, 26, 455-458.	4.0	57
78	Aerosol ultraviolet absorption experiment (2002 to 2004), part 2: absorption optical thickness, refractive index, and single scattering albedo. Optical Engineering, 2005, 44, 041005.	1.0	57
79	The February–March 2000 eruption of Hekla, Iceland from a satellite perspective. Geophysical Monograph Series, 2003, , 107-132.	0.1	56
80	SO <sub>2</sub> over central China: Measurements, numerical simulations and the tropospheric sulfur budget. Journal of Geophysical Research, 2012, 117, .	3.3	55
81	Ultraviolet optical model of volcanic clouds for remote sensing of ash and sulfur dioxide. Journal of Geophysical Research, 1997, 102, 21891-21904.	3.3	54
82	Fire at Iraqi sulfur plant emits SO2clouds detected by Earth Probe TOMS. Geophysical Research Letters, 2004, 31, .	4.0	52
83	Estimates of lightning NO <i><sub>x</sub></i> production based on OMI NO <sub>2</sub> observations over the Gulf of Mexico. Journal of Geophysical Research D: Atmospheres, 2016, 121, 8668-8691.	3.3	52
84	A Decade of Change in NO <sub>2</sub> and SO <sub>2</sub> over the Canadian Oil Sands As Seen from Space. Environmental Science & Technology, 2016, 50, 331-337.	10.0	52
85	Validation of ozone monitoring instrument SO <sub>2</sub> measurements in the Okmok volcanic cloud over Pullman, WA, July 2008. Journal of Geophysical Research, 2010, 115, .	3.3	50
86	Multi-source SO <sub>2</sub> emission retrievals and consistency of satellite and surface measurements with reported emissions. Atmospheric Chemistry and Physics, 2017, 17, 12597-12616.	4.9	50
87	Continuation of long-term global SO <sub>2</sub> pollution monitoring from OMI to OMPS. Atmospheric Measurement Techniques, 2017, 10, 1495-1509.	3.1	50
88	Global mapping of underwater UV irradiances and DNA-weighted exposures using Total Ozone Mapping Spectrometer and Sea-viewing Wide Field-of-view Sensor data products. Journal of Geophysical Research, 2001, 106, 27205-27219.	3.3	49
89	El Chichon: The genesis of volcanic sulfur dioxide monitoring from space. Journal of Volcanology and Geothermal Research, 2008, 175, 408-414.	2.1	49
90	Improving retrieval of volcanic sulfur dioxide from backscattered UV satellite observations. Geophysical Research Letters, 2009, 36, .	4.0	48

#	Article	IF	CITATIONS
91	International Photolysis Frequency Measurement and Model Intercomparison (IPMMI): Spectral actinic solar flux measurements and modeling. Journal of Geophysical Research, 2003, 108, .	3.3	47
92	Estimating the altitude of volcanic sulfur dioxide plumes from space borne hyperâ€spectral UV measurements. Geophysical Research Letters, 2009, 36, .	4.0	47
93	Comparison of satellite-derived UV irradiances with ground-based measurements at four European stations. Journal of Geophysical Research, 2006, 111, .	3.3	46
94	Relationship between column-density and surface mixing ratio: Statistical analysis of O3 and NO2 data from the July 2011 Maryland DISCOVER-AQ mission. Atmospheric Environment, 2014, 92, 429-441.	4.1	46
95	Comparison of OMI NO <sub>2</sub> observations and their seasonal and weekly cycles with ground-based measurements in Helsinki. Atmospheric Measurement Techniques, 2016, 9, 5203-5212.	3.1	46
96	Satelliteâ€based global volcanic SO <sub>2</sub> emissions and sulfate direct radiative forcing during 2005–2012. Journal of Geophysical Research D: Atmospheres, 2016, 121, 3446-3464.	3.3	45
97	Accounting for the effects of surface BRDF on satellite cloud andÂtrace-gas retrievals: aÂnew approach based on geometry-dependentÂLambertian equivalent reflectivityÂappliedÂtoÂOMIÂalgorithms. Atmospheric Measurement Techniques, 2017, 10, 333-349.	3.1	44
98	Version 2 total ozone mapping spectrometer ultraviolet algorithm: problems and enhancements. Optical Engineering, 2002, 41, 3028.	1.0	41
99	In situ measurements of tropospheric volcanic plumes in Ecuador and Colombia during TC <sup>4</sup> . Journal of Geophysical Research, 2011, 116, .	3.3	41
100	Comparison of UV irradiances from Aura/Ozone Monitoring Instrument (OMI) with Brewer measurements at El Arenosillo (Spain) – Part 1: Analysis of parameter influence. Atmospheric Chemistry and Physics, 2010, 10, 5979-5989.	4.9	40
101	A methodology to constrain carbon dioxide emissions from coal-fired power plants using satellite observations of co-emitted nitrogen dioxide. Atmospheric Chemistry and Physics, 2020, 20, 99-116.	4.9	40
102	Anthropogenic and volcanic point source SO <sub>2</sub> emissions derived from TROPOMI on board Sentinel-5 Precursor: first results. Atmospheric Chemistry and Physics, 2020, 20, 5591-5607.	4.9	39
103	Response of SO <sub>2</sub> and particulate air pollution to local and regional emission controls: A case study in Maryland. Earth's Future, 2016, 4, 94-109.	6.3	38
104	Highâ€resolution NO <sub>2</sub> observations from the Airborne Compact Atmospheric Mapper: Retrieval and validation. Journal of Geophysical Research D: Atmospheres, 2017, 122, 1953-1970.	3.3	38
105	Modeling of 2008 Kasatochi volcanic sulfate direct radiative forcing: assimilation of OMI SO <sub>2</sub> plume height data and comparison with MODIS and CALIOP observations. Atmospheric Chemistry and Physics, 2013, 13, 1895-1912.	4.9	37
106	Evaluation of GEOS-5 sulfur dioxide simulations during the Frostburg, MD 2010 field campaign. Atmospheric Chemistry and Physics, 2014, 14, 1929-1941.	4.9	37
107	Exploiting OMI NO2 satellite observations to infer fossil-fuel CO2 emissions from U.S. megacities. Science of the Total Environment, 2019, 695, 133805.	8.0	37
108	Satellite-derived emissions of carbon monoxide, ammonia, and nitrogen dioxide from the 2016 Horse River wildfire in the Fort McMurray area. Atmospheric Chemistry and Physics, 2019, 19, 2577-2599.	4.9	37

#	Article	IF	CITATIONS
109	Ultraviolet remote sensing of volcanic emissions. Geophysical Monograph Series, 2000, , 25-43.	0.1	35
110	Aerosol ultraviolet absorption experiment (2002 to 2004), part 1: ultraviolet multifilter rotating shadowband radiometer calibration and intercomparison with CIMEL sunphotometers. Optical Engineering, 2005, 44, 041004.	1.0	34
111	Transport and evolution of a pollution plume from northern China: A satelliteâ€based case study. Journal of Geophysical Research, 2010, 115, .	3.3	34
112	Anthropogenic sulphur dioxide load over China as observed from different satellite sensors. Atmospheric Environment, 2016, 145, 45-59.	4.1	33
113	Comparisons of spectral aerosol single scattering albedo in Seoul, South Korea. Atmospheric Measurement Techniques, 2018, 11, 2295-2311.	3.1	33
114	Assessment of NO <sub>2</sub> observations during DISCOVER-AQ and KORUS-AQ field campaigns. Atmospheric Measurement Techniques, 2020, 13, 2523-2546.	3.1	31
115	A new method for global retrievals of HCHO total columns from the Suomi National Polarâ€orbiting Partnership Ozone Mapping and Profiler Suite. Geophysical Research Letters, 2015, 42, 2515-2522.	4.0	30
116	Flux calculation using CARIBIC DOAS aircraft measurements: SO <sub>2</sub> emission of Norilsk. Journal of Geophysical Research, 2012, 117, .	3.3	29
117	First estimates of global free-tropospheric NO <sub>2</sub> abundances derived using a cloud-slicing technique applied to satellite observations from the Aura Ozone Monitoring Instrument (OMI). Atmospheric Chemistry and Physics, 2014, 14, 10565-10588.	4.9	29
118	Satellite observation of pollutant emissions from gas flaring activities near the Arctic. Atmospheric Environment, 2016, 133, 1-11.	4.1	29
119	Comparisons between ground measurements of broadband ultraviolet irradiance (300 to 380 nm) and total ozone mapping spectrometer ultraviolet estimates at Moscow from 1979 to 2000. Optical Engineering, 2002, 41, 3070.	1.0	28
120	Comparison of UV irradiances from Aura/Ozone Monitoring Instrument (OMI) with Brewer measurements at El Arenosillo (Spain) – Part 2: Analysis of site aerosol influence. Atmospheric Chemistry and Physics, 2010, 10, 11867-11880.	4.9	28
121	Version 2 Ozone Monitoring Instrument SO <sub>2</sub> product (OMSO2) Tj ET Atmospheric Measurement Techniques, 2020, 13, 6175-6191.	Qq1 1 0.7 3.1	'84314 rgBT 27
122	Airborne MAXâ€ÐOAS measurements over California: Testing the NASA OMI tropospheric NO <sub>2</sub> product. Journal of Geophysical Research D: Atmospheres, 2013, 118, 7400-7413.	3.3	26
123	Five decades observing Earth's atmospheric trace gases using ultraviolet and visible backscatter solar radiation from space. Journal of Quantitative Spectroscopy and Radiative Transfer, 2019, 238, 106478.	2.3	26
124	Study of SO Pollution in the Middle East Using MERRAâ€2, CAMS Data Assimilation Products, and Highâ€Resolution WRFâ€Chem Simulations. Journal of Geophysical Research D: Atmospheres, 2020, 125, e2019JD031993.	3.3	26
125	A new approach to estimating the albedo for snow-covered surfaces in the satellite UV method. Journal of Geophysical Research, 2003, 108, .	3.3	25
126	Midlatitude Lightning NO <sub>x</sub> Production Efficiency Inferred From OMI and WWLLN Data. Journal of Geophysical Research D: Atmospheres, 2019, 124, 13475-13497.	3.3	25

Νιςκοίας Α Κrotkov

#	Article	IF	CITATIONS
127	Characterization of OMI tropospheric NO <sub>2</sub> over the Baltic Sea region. Atmospheric Chemistry and Physics, 2014, 14, 7795-7805.	4.9	24
128	Comparison of operational satellite SO <sub>2</sub> products with ground-based observations in northern Finland during the Icelandic Holuhraun fissure eruption. Atmospheric Measurement Techniques, 2015, 8, 2279-2289.	3.1	24
129	First Observations of Volcanic Eruption Clouds From the L1 Earthâ€&un Lagrange Point by DSCOVR/EPIC. Geophysical Research Letters, 2018, 45, 11,456.	4.0	23
130	The TROPOMI surface UV algorithm. Atmospheric Measurement Techniques, 2018, 11, 997-1008.	3.1	23
131	Problems in assessment of the ultraviolet penetration into natural waters from space-based measurements. Optical Engineering, 2002, 41, 3019.	1.0	21
132	Applications of Satellite-Based Sulfur Dioxide Monitoring. IEEE Journal of Selected Topics in Applied Earth Observations and Remote Sensing, 2009, 2, 293-298.	4.9	21
133	Rapid transpacific transport in autumn observed by the Aâ€ŧrain satellites. Journal of Geophysical Research, 2012, 117, .	3.3	21
134	A cloud algorithm based on the O <sub>2</sub> -O <sub>2</sub> 477 nm absorption band featuring an advanced spectral fitting method and the use of surface geometry-dependent Lambertian-equivalent reflectivity. Atmospheric Measurement Techniques, 2018, 11, 4093-4107.	3.1	21
135	Retrieval of ozone column from global irradiance measurements and comparison with TOMS data. A year of data in the Alps. Geophysical Research Letters, 2002, 29, 23-1-23-4.	4.0	20
136	Optical, microphysical and compositional properties of the Eyjafjallajökull volcanic ash. Atmospheric Chemistry and Physics, 2014, 14, 10649-10661.	4.9	20
137	A geometry-dependent surface Lambertian-equivalent reflectivity product for UV–Vis retrievals – Part 1: Evaluation over land surfaces using measurements from OMI at 466 nm. Atmospheric Measurement Techniques, 2019, 12, 3997-4017.	3.1	19
138	A sulfur dioxide Covariance-Based Retrieval Algorithm (COBRA): application to TROPOMI reveals new emission sources. Atmospheric Chemistry and Physics, 2021, 21, 16727-16744.	4.9	19
139	Total ozone mapping spectrometer retrievals of noon erythemal-CIE ultraviolet irradiance compared with Brewer ground-based measurements at El Arenosillo (southwestern Spain). Journal of Geophysical Research, 2007, 112, .	3.3	18
140	Ceramic industry at Morbi as a large source of SO2 emissions in India. Atmospheric Environment, 2020, 223, 117243.	4.1	18
141	Tracking aerosols and SO <sub>2</sub> clouds from the Raikoke eruption: 3D view from satellite observations. Atmospheric Measurement Techniques, 2021, 14, 7545-7563.	3.1	18
142	Lightning NO <sub>x</sub> Production in the Tropics as Determined Using OMI NO <sub>2</sub> Retrievals and WWLLN Stroke Data. Journal of Geophysical Research D: Atmospheres, 2019, 124, 13498-13518.	3.3	17
143	The GeoTASO airborne spectrometer project. Proceedings of SPIE, 2014, , .	0.8	16
144	Quantifying urban, industrial, and background changes in NO <sub>2</sub> during the COVID-19 lockdown period based on TROPOMI satellite observations. Atmospheric Chemistry and Physics, 2022, 22, 4201-4236.	4.9	16

#	ARTICLE	IF	CITATIONS
145	Surface erythemal UVÂirradiance in the continental United States derived from ground-based and OMI observations: quality assessment, trend analysis and sampling issues. Atmospheric Chemistry and Physics, 2019, 19, 2165-2181.	4.9	15
146	A Balloon Sounding Technique for Measuring SO2 Plumes. Journal of Atmospheric and Oceanic Technology, 2010, 27, 1318-1330.	1.3	14
147	Likely seeding of cirrus clouds by stratospheric Kasatochi volcanic aerosol particles near a mid-latitude tropopause fold. Atmospheric Environment, 2012, 46, 441-448.	4.1	14
148	Ultraviolet Satellite Measurements ofÂVolcanicÂAsh. , 2016, , 217-231.		14
149	Using CATS nearâ€realâ€time lidar observations to monitor and constrain volcanic sulfur dioxide (SO <sub>2</sub> ) forecasts. Geophysical Research Letters, 2016, 43, 11,089.	4.0	14
150	Linking improvements in sulfur dioxide emissions to decreasing sulfate wet deposition by combining satellite and surface observations with trajectory analysis. Atmospheric Environment, 2019, 199, 210-223.	4.1	14
151	TEMPO Green Paper: Chemistry, physics, and meteorology experiments with the Tropospheric Emissions: monitoring of pollution instrument. , 2019, , .		14
152	<title>Comparisons of USDA UV shadow-band irradiance measurements with TOMS satellite and DISORT model retrievels under all sky conditions</title> . , 2002, , .		13
153	A geometry-dependent surface Lambertian-equivalent reflectivity product for UV–Vis retrievals – Part 2: Evaluation over open ocean. Atmospheric Measurement Techniques, 2019, 12, 6749-6769.	3.1	13
154	Description and validation of the OMI very fast delivery products. Journal of Geophysical Research, 2008, 113, .	3.3	12
155	Revised and extended benchmark results for Rayleigh scattering of sunlight in spherical atmospheres. Journal of Quantitative Spectroscopy and Radiative Transfer, 2020, 254, 107181.	2.3	12
156	VolKilau: Volcano Rapid Response Balloon Campaign during the 2018 Kilauea Eruption. Bulletin of the American Meteorological Society, 2020, 101, E1602-E1618.	3.3	12
157	A new discrete wavelength backscattered ultraviolet algorithm for consistent volcanic SO <sub>2</sub> retrievals from multiple satellite missions. Atmospheric Measurement Techniques, 2019, 12, 5137-5153.	3.1	12
158	Application of satellite-based sulfur dioxide observations to support the cleantech sector: Detecting emission reduction from copper smelters. Environmental Technology and Innovation, 2018, 12, 172-179.	6.1	11
159	Inconsistencies in sulfur dioxide emissions from the Canadian oil sands and potential implications. Environmental Research Letters, 2021, 16, 014012.	5.2	11
160	Partitioning between aerosol and NO 2 absorption in the UV spectral region. , 2005, 5886, 588601.		10
161	High-resolution mapping of SO2 using airborne observations from the GeoTASO instrument during the KORUS-AQ field study: PCA-based vertical column retrievals. Remote Sensing of Environment, 2020, 241, 111725.	11.0	10
162	Influence of desert dust intrusions on groundâ€based and satelliteâ€derived ultraviolet irradiance in southeastern Spain. Journal of Geophysical Research, 2012, 117, .	3.3	9

#	Article	IF	CITATIONS
163	Limb–nadir matching using non-coincident NO <sub>2</sub> observations: proof of concept and the OMI-minus-OSIRIS prototype product. Atmospheric Measurement Techniques, 2016, 9, 4103-4122.	3.1	9
164	<title>Version 2 TOMS UV algorithm: problems and enhancements</title> . , 2002, 4482, 82.		8
165	Long-term UV irradiance changes over Moscow and comparisons with UV estimates from TOMS and METEOSAT. , 2005, 5886, 83.		8
166	SO2 trajectories in a complex terrain environment using CALPUFF dispersion model, OMI and MODIS data. International Journal of Applied Earth Observation and Geoinformation, 2018, 69, 99-109.	2.8	8
167	Global distribution and 14-year changes in erythemal irradiance, UV atmospheric transmission, and total column ozone for2005–2018 estimated from OMI and EPIC observations. Atmospheric Chemistry and Physics, 2020, 20, 8351-8380.	4.9	8
168	Ground-based retrievals of aerosol column absorption in the UV spectral region and their implications for GEMS measurements. Remote Sensing of Environment, 2020, 245, 111759.	11.0	7
169	Geophysicists unite to validate volcanic SO2measurements. Eos, 1997, 78, 217-223.	0.1	6
170	<title>Problems in assessment of the UV penetration into natural waters from space-based measurements</title> . , 2002, , .		6
171	Deriving aerosol parameters from absolute UV sky radiance measurements using a Brewer double spectrometer. , 2003, 5156, 323.		6
172	A new technique for retrieval of tropospheric and stratospheric ozone profiles using sky radiance measurements at multiple view angles: Application to a Brewer spectrometer. Journal of Geophysical Research, 2008, 113, .	3.3	6
173	Aerosol column absorption measurements using co-located UV-MFRSR and AERONET CIMEL instruments. , 2009, , .		6
174	Comparison of TOMS retrievals and UVMRP measurements of surface spectral UV radiation in the United States. Atmospheric Chemistry and Physics, 2010, 10, 8669-8683.	4.9	6
175	Reduction of skylight reflection effects in the above-water measurement of diffuse marine reflectance: comment. Applied Optics, 2000, 39, 1379.	2.1	5
176	Chemical climatology of atmospheric pollutants in the eastern United States: Seasonal/diurnal cycles and contrast under clear/cloudy conditions for remote sensing. Atmospheric Environment, 2019, 206, 85-107.	4.1	5
177	Explicit and consistent aerosol correction for visible wavelength satellite cloud and nitrogen dioxide retrievals based on optical properties from a global aerosol analysis. Atmospheric Measurement Techniques, 2021, 14, 2857-2871.	3.1	5
178	Volcanic SO <sub>2</sub> effective layer height retrieval for the Ozone Monitoring Instrument (OMI) using a machine-learning approach. Atmospheric Measurement Techniques, 2021, 14, 3673-3691.	3.1	5
179	Numerical results for polarized light scattering in a spherical atmosphere. Journal of Quantitative Spectroscopy and Radiative Transfer, 2022, 287, 108194.	2.3	5
180	<title>Comparison of Brewer UV irradiance measurements with TOMS satellite retrievals</title> . , 2002, , .		4

Νιςκοίας Α Κrotkov

1

#	Article	IF	CITATIONS
181	Enhanced monitoring of sulfur dioxide sources with hyperspectral UV sensors. , 2009, , .		4
182	A New Database Program for Spectral Surface UV Measurements. Journal of Atmospheric and Oceanic Technology, 1996, 13, 1291-1299.	1.3	3
183	Assessment of TOMS UV bias due to absorbing aerosols. , 2004, , .		3
184	The net decay time of anomalies in concentrations of atmospheric pollutants. Atmospheric Environment, 2017, 160, 19-26.	4.1	3
185	Advances in UV Satellite Monitoring of Volcanic Emissions. , 2021, , .		3
186	Day–Night Monitoring of Volcanic SO2 and Ash Clouds for Aviation Avoidance at Northern Polar Latitudes. Remote Sensing, 2021, 13, 4003.	4.0	3
187	Use of Hyper-Spectral Visible and Near-Infrared Satellite Data for Timely Estimates of the Earth's Surface Reflectance in Cloudy and Aerosol Loaded Conditions: Part 1–Application to RGB Image Restoration Over Land With GOME-2. Frontiers in Remote Sensing, 2022, 2, .	3.5	3
188	<title>Optimization of the polarization remote-sensing techniques of the ocean</title> . , 1992, , .		2
189	<title>Comparisons between ground measurements of UV irradiance 290 to 380nm and TOMS UV&lt;br&gt;estimates over Moscow for 1979-2000</title> . , 2002, , .		2
190	Measuring aerosol UV absorption optical thickness by combining use of shadowband and almucantar techniques. , 2004, , .		2
191	Retrieval of volcanic SO <sub>2</sub> from HIRS/2 using optimal estimation. Atmospheric Measurement Techniques, 2017, 10, 2687-2702.	3.1	2
192	Rethinking the correction for absorbing aerosols in the OMI- and TROPOMI-like surface UV algorithms. Atmospheric Measurement Techniques, 2021, 14, 4947-4957.	3.1	2
193	Using Machine Learning for Timely Estimates of Ocean Color Information From Hyperspectral Satellite Measurements in the Presence of Clouds, Aerosols, and Sunglint. Frontiers in Remote Sensing, 2022, 3,	3.5	2
194	<title>Simulation of the thermospheric infrared emissions in the aurora</title> . , 1993, 2049, 256.		1
195	<title>Ultraviolet radiation in the atmosphere-ocean system: a model study</title> . , 1993, , .		1
196	Goddard UV aerosol absorption closure experiment (2002-03). , 2003, 5156, 54.		1
197	Real Time Volcanic Cloud Products and Predictions for Aviation Alerts. , 2014, , .		1

198 CHAPS: a sustainable approach to targeted air pollution observation from small satellites. , 2021, , .

#	Article	IF	CITATIONS
199	Estimates of Hyperspectral Surface and Underwater UV Planar and Scalar Irradiances from OMI Measurements and Radiative Transfer Computations. Remote Sensing, 2022, 14, 2278.	4.0	1
200	<title>Estimation of the uncertainties of the retrieved seawater parameters</title> ., 1993, , .		0
201	Estimating UV index climatology over North America. , 2003, , .		0
202	Characterization and error analysis of an operational retrieval algorithm for estimating column ozone and aerosol properties from ground-based ultra-violet irradiance measurements. , 2005, , .		0
203	UV aerosol optical properties at three US sites. , 2005, 5979, 492.		Ο
204	Spectral distribution of UV-B irradiance derived by synthetic model compared with simulation results of TUV and ground measurements. , 2006, 6298, 153.		0
205	Validation of TOMS UV irradiance with Brewer ground-based measurements at southwestern Spain. , 2006, , .		0
206	The CLEO spectrometer system: first results. Proceedings of SPIE, 2009, , .	0.8	0
207	Aerosol single scattering albedo retrieval with various techniques in the UV and visible wavelength range. , 2009, , .		0
208	Applying the OMI NO2 Retrieval Algorithm to Estimate the Production Efficiency of Lightning NOx. , 2016, , .		0
209	Hit from Both Sides. , 2011, , 75-108.		Ο
210	Filling the Gaps: The Synergistic Application of Satellite Data for the Volcanic Ash Threat to Aviation. , 2013, , .		0